Curvature Effects on Compressive Failure Strength of Long Fiber Composite Laminates

K. J. HSIA* AND J. Q. HUANG

Department of Theoretical and Applied Mechanics

University of Illinois at Urbana-Champaign

Urbana, IL 61801

November 1992

K. J. Hsia* Assistant Professor
Department of Theoretical and Applied Mechanics
University of Illinois at Urbana-Champaign
Urbana, IL 61801
(217)333-2321, fax: (217)244-5707

J. Q. Huang Visiting Assistant Professor
Department of Theoretical and Applied Mechanics
University of Illinois at Urbana-Champaign
Urbana, IL 61801
(217)333-3294

* To whom correspondence and proofs should be sent.

ABSTRACT

A simple model is developed to study the compressive failure strength of woven composite laminates. Two different configurations, a flat plate under in-plane compression and a thin-walled cylindrical tube under external pressure, are considered. Two micromechanisms observed in experiments, delamination of thin layers at the inner surface for the tube and formation of kinking bands for the flat plate, are used to develop the model. An energy criterion is employed to determine the failure strength of cylindrical tube. Three nondimensional parameters, related to interlayer surface energy, initial misalignment of fibers, and the delaminated layer thickness as well as the radius of curvature of the tube, are identified as governing parameters for different failure modes. The model predictions agree well with experimental results.

Key words: woven composites, compressive strength, kinking, delamination.

1. INTRODUCTION

It has been widely observed that, in long fiber composite laminates such as unidirectional and woven composites, the compressive failure strength is usually lower than the tensile failure strength. However, compressive strength is often the design limiting criterion in many applications. It is well established that compressive failure of composite laminates can be attributed to one of many different micromechanisms, including: elastic microbuckling [1], formation of kink bands or plastic microbuckling [2-6], fiber collapse [7-9], and inter-layer delamination [10-15, 6]. Whichever of these mechanisms gives the lowest compressive failure stress will dominate the failure process.

What makes the problem more complicated is that the failure stresses due to different mechanisms will not only depend on the intrinsic properties of composites such as constituents properties and microstructures, but also on the external conditions such as loading types, specimen geometries, and boundary conditions [16]. Wang and Socie [6] made an interesting observation that, in woven composites, the compressive failure stress of a thin-walled tube under external pressure is only about one half of that of a flat plate under in-plane compression. A detailed study of failure surfaces revealed that the failure mechanism of the flat plate was formation of kink bands, whereas the mechanism of the cylindrical tube was delamination caused by buckling of layers at inner surface.

In the present paper, based on the mechanisms of the compressive failure of composite laminates, we will develop a simple model for delamination failure of cylindrical tubes. We will concentrate on unidirectional and woven composite laminates without macroscopic stress concentrators such as notches and holes. A number of non-dimensional parameters which determine the final compressive strength of woven composite tubes will be identified. Models of the compressive strength of flat composite plate due to formation of kink bands will also be reviewed. The results will be compared with the experimental measurements.

2. DELAMINATION FAILURE OF CYLINDRICAL TUBES

Delamination failure of a cylindrical tube under external pressure is often caused by buckling of one or several layers at the inner surface of the composites, as those shown in Fig. 1. It was

also shown by Tarnopl'skii and Kincis [12] that buckling could occur progressively layer by layer at the inner surface in a thick-walled tube, apparently due to nonuniform stress distribution in the tube (the compressive stress is higher at the inner radius). In the following, we consider only a thin-walled cylindrical tube under external compression. Instead of analyzing the detailed process of delamination which requires interfacial fracture analysis, we study only the states before and after the buckling occurs, and calculate the total energy of these states by assuming an approximate deflection shape for the post-buckling mode, thus to provide an estimate of the driving force for delamination.

In the current analysis, we assume that the width of the buckled layer along axial direction of the tube is sufficiently large so that a stripe of unit width in the middle region of the buckled layer can be considered as a curved beam with an initial radius of curvature R_0, where R_0 is the inner radius of the tube plus one half of the height of the buckled layer. A curvilinear coordinate system, s, shown in Fig.1 is chosen. we denote the height of the buckled layer by t, length of the buckled portion by l, and consider only unit width.

To simplify the mathematical derivation, some approximations are made. The deformation is assumed to be small so that the change of radius due to axisymmetrical compression is considered to be negligible compare to the radius itself, i.e., $R \cong R_0$.

Strain energy of stay in plane deformation. When the deformation of the layer stays in the original plane of the cylindrical tube, the total strain energy of a curved beam of unit width (see Fig. 1) under compressive stress σ is given as

$$U_{stay} = \frac{\sigma^2 t l}{2E} \quad , \tag{1}$$

where E is the Young's modulus in the direction parallel to the compressive stress.

Total energy of buckled layer. The total energy of the buckled layer consists of two parts,

$$U_{buckle} = U_1 + U_2 \quad , \tag{2}$$

where U_1 is the energy per unit width due to generation of new surfaces, and U_2 is the strain energy per unit width of the deflected beam. It is easily seen that

$$U_1 = 2\gamma l \quad , \tag{3}$$

where γ is the interlaminar surface energy in units of J/m^2.

To estimate the strain energy, U_2, we assume that the strain energy due to extensional deformation is negligible compared to the strain energy due to bending, i.e.,

$$U_2 = \frac{1}{2}\int_l \frac{M^2(s)}{EI} ds \tag{4}$$

where $I=t^3/12$ is the moment of inertia of the beam cross-section. M(s) is the bending moment in the curved beam, and is related to the deflection $v(s)$ by (see Oden [17]),

$$-\frac{M}{EI} = \frac{d^2v}{ds^2} + \frac{v}{R^2} \tag{5}$$

The deflection of the buckled layer, in the direction normal to the original neutral axis of the beam and pointing inward, can be assumed to take the form,

$$v(s) = \frac{v_0}{2}(\cos(\frac{2\pi s}{l}) + 1) + v_1 \quad , \tag{6}$$

where $v_1=\sigma R_0/E$ is the uniform displacement of the tube due to the uniform compressive stress σ. The amplitude v_0 can be determined by the compatibility condition between the buckled and unbuckled portion of the tube, i.e., the displacement at the end ($s=l/2$) of the buckled beam along s-direction must be the same as that of the unbuckled beam, and the length of the delaminated section remains unchanged. This condition leads to

$$\frac{\sigma}{E}\frac{l}{2} = \frac{1}{2}\int_0^{l/2} (\frac{dv}{ds})^2 ds, \tag{7}$$

or,

$$v_0^2 = \frac{\sigma}{E}(\frac{2l}{\pi})^2 \quad . \tag{8}$$

Using the deflection function v(s) in (6), and equations (2-8), the total energy of the buckled layer per unit width can be obtained as

$$U_{buckle} = Et^2\{\left[1-(\frac{1}{2\pi}\xi\bar{l})^2\right]^2\frac{\pi^2}{3\bar{l}}\bar{\sigma}+\frac{1}{24}\xi^4\bar{l}(\sqrt{\bar{\sigma}}\frac{\bar{l}}{\pi}+\frac{\bar{\sigma}}{\xi})^2+2\bar{\gamma}\bar{l}\} \quad , \tag{9}$$

where we define the non-dimensional parameters as,

$$\bar{\sigma}=\frac{\sigma}{E},\ \bar{\gamma}=\frac{\gamma}{Et},\ \bar{l}=\frac{l}{t},\ \text{and}\ \xi=\frac{t}{R_0}\ . \tag{10}$$

Criterion for delamination. It is conceivable that delamination will occur when the total energy of the buckled layer is smaller than or equal to the strain energy of the stay in plane layer, which first happens when $U_{buckle}=U_{stay}$. Therefore, the critical stress at delamination, $\bar{\sigma}_c$, is determined by equating (1) to (9), which gives,

$$\bar{\sigma}_c^2=\left[1-(\frac{1}{2\pi}\xi\bar{l})^2\right]^2\frac{2\pi^2}{3(\bar{l})^2}\bar{\sigma}_c+\frac{1}{12}\xi^4(\sqrt{\bar{\sigma}_c}\frac{\bar{l}}{\pi}+\frac{\bar{\sigma}_c}{\xi})^2+4\bar{\gamma} \quad . \tag{11}$$

It should be noted that the delamination length $\bar{l}$ in (11) is not specified. Obviously, a length which gives a minimum value of delamination stress is preferred. Therefore, the critical delamination stress in (11) can be defined as the lowest stress for any delamination length $\bar{l}$. Once delamination occurs, it is assumed that the load bearing capacity of the tube is nearly exhausted. Thus the critical delamination stress can be considered as the compressive strength of the composite tube.

A typical normalized stress $\bar{\sigma}$ vs. normalized length $\bar{l}$ curve is shown in Fig. 2, which demonstrates that a minimum stress exists. In this plot, nondimensional parameters t/R_0=0.02, $\bar{\gamma}/(Et)=10^{-5}$ were used. For typical values of E=20 GPa, t/R_0=0.02, and $\bar{\gamma}/(Et)=10^{-5}$ and 10^{-4}, the delamination stresses are 128 MPa and 400 MPa, respectively.

3. FAILURE OF FLAT PLATE DUE TO FORMATION OF KINK BANDS

Another common failure mechanism of composite laminates is the formation of kinking bands, as shown schematically in Fig. 3. It has been shown by Fleck and Budiansky [9] that the mechanism of kinking failure in unidirectional fiber composites is usually plastic microbuckling.

Efforts have been made to calculate the critical stress at which kinking occurs. Assuming a rigid-perfectly plastic behavior in shear for unidirectional long fiber composites, Argon [2]

obtained a critical compressive stress as

$$\sigma_c = \frac{\tau_y}{\phi} \quad , \tag{12}$$

where τ_y is the shear yield strength in the direction parallel to the fibers, and ϕ is the angle of initial misalignment of fibers. This result was later extended by Budiansky [3] to an elastic-perfectly plastic composite, for which the critical kinking stress is

$$\sigma_c = \frac{\tau_y}{\gamma_y + \phi} = \frac{G}{1 + \phi/\gamma_y} \quad , \tag{13}$$

where G is the shear modulus in the direction parallel to the fibers which is often about 1/7 of the corresponding Young's modulus, γ_y is the shear yield strain. Typical value of ϕ/γ_y ranges from 2 to 8 for unidirectional fiber composites (see Budiansky and Fleck [4]).

Taking $G=E/\alpha$ ($\alpha \approx 7$), the normalized compressive strength due to kinking is given as,

$$\bar{\sigma}_c = \frac{1}{\alpha(1 + \phi/\gamma_y)} \quad . \tag{14}$$

Obviously, for any given material with given shear modulus G and initial waviness ϕ/γ_y, the compressive strength along the fiber direction of the composite is a constant.

Failure by forming of kinking bands has also been observed by Wang and Socie [6] in their flat plate specimens. They found that under bi-axial stress in woven composite flat plate, regardless of the level of secondary compression (the stress with a lower magnitude), the compressive failure stress is always about 320 MPa. This result is consistent with the predictions by the models of kinking failure described above, since kinking failure criterion requires only that local shear yielding condition be reached in one direction (along fiber direction) regardless of stresses in other directions.

4. RESULTS AND DISCUSSION

With the two failure mechanisms of composite laminates analyzed, the failure stress for a given long fiber composite and a given specimen geometry can then be determined. The failure stress due to delamination given by equations (11) is a function of the normalized surface energy, $\bar{\gamma}$, and the ratio of the delaminated layer thickness to the radius of curvature, t/R_0. Whereas the

failure stress due to formation of kink bands given by equation (14) will only be dependent on the initial waviness of fibers and the yield strength of matrix, and independent of $\bar{\gamma}$ and t/R_0.

The normalized delamination stress is shown in Fig.4 as a function of the normalized interlaminar surface energy for typical values of t/R_0=0.1 and 0.01. As expected, the delamination stress increases with the fracture surface energy, i.e., a higher surface energy requires a larger stress to reach the delamination condition. On the other hand, the delamination stress has a relatively weak dependence on the thickness-to-radius ratio t/R_0. The results also indicate that the delamination stress increases with increasing t/R_0, i.e., the thicker the relative thickness t/R_0, the higher the delamination stress will be.

Fig.5 shows the normalized kinking failure stress verses the normalized misalignment parameter, ϕ/γ_y, where the shear modulus G is taken to be $E/7$. The plot shows that kinking failure strength is very sensitive to the initial misalignment, particularly when the misalignment angle is small. In real material, there exists a statistical distribution misalignment angle. Therefore, kinking failure usually initiates at locations where misalignment angle peaks.

Plotting the compressive strengths due to two different mechanisms together, Fig. 6, we can see that the two failure mechanisms compete with each other. When interlaminar surface energy is low, delamination failure is likely to be the failure mode; but when interlaminar surface energy is beyond a critical value (shown in Fig. 6), kinking failure is preferred. The critical value of interlaminar energy is dependent on both the thickness-to-radius ratio t/R_0 and the misalignment parameter ϕ/γ_y. Fig. 6 shows that, for a fixed ratio t/R_0, critical interlaminar energy increases with decreasing misalignment. It can be easily shown that critical interlaminar energy would decrease with increasing t/R_0. Kinking failure strength, determined by the parameter ϕ/γ_y, sets the ultimate ceiling of composite compressive strength regardless of the specimen geometry.

Based on the current model, a failure mechanisms map can be constructed in a space characterized by material properties, i.e., ϕ/γ_y - $\bar{\gamma}$ space. Such a map is shown in Fig. 7, which shows that materials with large misalignment and high interfacial energy tend to fail by formation of kinking bands, whereas those with small misalignment and low interfacial energy are likely to fail by delamination. The effect of the geometrical parameter, t/R_0, is to shift the dividing curve of dominant failure modes.

As a special case, our model predictions are compared with the experimental results

obtained by Wang and Socie [6]. The material tested by them is a glass fiber, NEMA/ASTM G-10 grade woven composite laminates. The material properties are given in Table 1. The only unknown material parameter for this material is the interlayer surface energy γ. However, it was measured by other people on some similar polymeric matrix materials that the interlayer surface energy was reported to be around 130-150 J/m^2 for regularly cured laminates [18, 19].

The critical failure stresses measured by Wang and Socie for two test configurations, a flat plate and a cylindrical tube, were 320 MPa and 170 MPa, respectively. The compressive failure mechanism of the flat plate was found to be formation of kink bands and that of the cylindrical tube was delamination of one or a few layers on the inner surface. The initial misalignment angle, ϕ, of the woven composite was reported to be less than 10^o. Using equation (14) and the kinking failure stress of 320 MPa together with the measured material properties, we can determine that the initial misalignment angle is about ϕ=4.5^o for the tested composite.

The delamination stresses for the observed layer thickness t=0.5 mm were calculated based on the present model. For the typical range of the surface energy γ=130-150 J/m^2, the delamination stresses are in the range of 155-167 MPa, which agree very well with the measured value of the delamination stress 170 MPa.

5. CONCLUDING REMARKS

A simple model has been developed in this paper based on the failure mechanisms observed in experiments. Both the compressive failure mode due to formation of kink bands and the mode due to delamination are considered. Despite the approximations, the results show that the model can explain the effects of specimen geometry on the compressive failure stress of long fiber composites. The model predictions agree with the experimental results of Wang and Socie [6] rather well.

Three non-dimensional groups are identified by the model as governing parameters for compressive failure mechanisms of composite laminates: the normalized interlayer surface energy, γ/Et; the ratio of the delaminated layer thickness to the initial radius of curvature, t/R_0; and the ratio of the initial misalignment angle to the matrix shear strain at yielding, ϕ/γ_y. Our results indicate that the two mechanisms, delamination and kinking, compete with each other to determine the final failure strength of the composite. If delamination is the dominant failure mecha-

nism, the interlayer surface energy γ is the key parameter which controls the delamination stress. On the other hand, when kinking failure dominates, the way to improve the composites compressive strength is to reduce the initial misalignment angle ϕ and increase the material's shear yield strength. The upper bound to the compressive strength is set by the kinking failure stress.

Real failure processes of composites are not as ideal as we considered here. Neither delamination nor kinking failure will occur instantaneously over the whole specimen. They usually initiate from some processing defects within the material (interlayer bubbles, dirt, or heavily misaligned regions) and then propagate through the specimen to result in final failure. Therefore, an effective way to control the propagation of kink bands and delamination may also raise the compressive failure strength. On the other hand, failure process in composites is never a clear-cut process. Even for the flat plate, a close examination of specimens tested by Wang and Socie [6] reveals that while major portion of the failure plane is kinking failure, some portion still shows traces of delamination. Furthermore, uniform stress distributions are rarely encountered in engineering applications. Holes and notches are inevitable in engineering components. Since the mechanical behaviors of composite materials are geometry sensitive, problems of composite materials with stress concentrators must be considered with special care as was done by Suo, *et al.* [20] for ceramic-matrix fiber composites.

ACKNOWLEDGEMENTS

This work is supported by the University of Illinois at Urbana-Champaign. KJH is also partly supported by NSF grant MSS 92-09309. We are grateful to the helpful discussions with Prof. D. F. Socie and Dr. J. Z. Wang of the University of Illinois and the experimental data provided by them.

REFERENCES

1. B.W. Rosen, "Mechanics of Composite Strengthening", in Fiber Composite Materials, Am. Soc. Metals Seminar, pp. 37-75 (1965).

2. A. S. Argon, "Fracture of Composites", in Treatise on Materials Science and Technology, Volume 1, Edited by H. Herman, pp. 79-114 (1972).

3. B. Budiansky, "Micromechanics", *Computers and Structures*, 16(1), pp. 3-12 (1983).

4. B. Budiansky and N. A. Fleck, "Compressive Failure of Fiber Composites", submitted to *J. Mech. Phys. Solids*.

5. A. G. Evans and W. F. Adler, "Kinking as a Mode of Structural Degradation in Carbon Fiber Composites", *Acta Metall.*, 26, pp. 725-738 (1978).

6. J. Z. Wang and D. F. Socie, "Failure Strength and Damage Mechanisms of E-Glass/Epoxy Laminates Under In-Plane Biaxial Compressive Deformation", *J. Composite Mat.*, in press.

7. P. D. Ewins and R. T. Potter, "Some Observations on the Nature of Fiber Reinforced Plastics and the Implications for Structural Design", *Phil. Trans. R. Soc. London*, A294, pp. 507-517 (1980).

8. M. R. Piggott and B. Harris, "Compression Strength of Carbon, Glass and Kevlar-49 Fiber Reinforced Polyester Resins", *J. Mat. Sci.*, 15, pp. 2523-2538 (1980).

9. N. A. Fleck and B. Budiansky, "Compressive Failure of Fiber Composites due to Microbuckling", *Proc. IUTAM Symp. on Inelastic Deformation of Composite Materials*, Troy, New York, May 29-June 1, 1990, Edited by J. Dvorak, pp. 235-273, Springer-Verlag (1991).

10. L. M. Kachanov, "Separation of Composite Materials", *Mekh. Polim.*, No. 5, pp. 918-922 (1976).

11. H. Chai, W. G. Knauss and C. D. Babcock, "Observation of Damage Growth in Compressively Loaded Laminates", *Experimental Mechanics*, 23(3), p. 329 (1983).

12. Yu. M. Tarnopl'skii and T. Kincis, "Methods of Static Testing for Composites", in Handbook of Composites, Vol. 3: Failure Mechanics of Composites, Edited by G.C. Sih and A.M. Skudra, pp. 215-275 (1985).

13. L. M. Kachanov, "Delamination Buckling of Composite Materials", Kluwer Academic Publishers (1988).

14. W. J. Bottega and A. Maewal, "Delamination Buckling and Growth in Laminates", *Journal of Applied Mechanics*, 50, pp. 184-189 (1983).

15. S. S. Wang, N. M. Zahlan and H. Suemasu, "Compressive Stability of Delaminated Random Short-Fiber Composites, Part I ---- Modelling and Methods of Analysis", *Journal of Com-*

posite Materials, 19, pp. 297-316 (1985).

16. J. Z. Wang, "Failure Strength and Mechanism of Composite Laminates Under Multiaxial Loading Conditions", PhD Thesis, Department of Mechanical Engineering, University of Illinois at Urbana-Champaign, 1992.

17. J. T. Oden, "Mechanics of Elastic Structures", McGRAW-HILL Book Company (1967).

18. C. E. Browning and H. S. Schwartz, "Delamination Resistant Composite Concepts", in Composite Materials: Testing and Design (Seventh Conference). ASTM STP 893, J. M. Whitney, Ed., American Society for Testing and Materials, Philadelphia, pp. 256-265 (1986).

19. H. Chai, C. D. Babcock and W. G. Knauss, "One Dimensional Modelling of Failure in Laminated Plates by Delamination Buckling", *Int. J. Solids Structures*, 17, No. 11, pp. 1069-1083 (1981).

20. Z. Suo, S. Ho and X. Gong, "Notch Ductile-to-Brittle Transition due to Localized Inelastic Band", to be published

Table 1: Material Properties and Geometry of G-10 Composite Specimens

Properties	Values
Young's Modulus E	22.8×10^3 (MPa)
Shear Modulus G	2.9×10^3(MPa)
Shear Yield Strain γ_y	0.01
Compressive Strength	- 332 (MPa)
Compressive Failure Strain	-0.016
Inner Radius of the Tube	22.5 (mm)
Thickness of the Buckled Layer	0.5 (mm)

FIGURE CAPTIONS

Fig. 1 Delamination failure mode of a thin-walled tube under external pressure.

Fig. 2 A typical curve of the normalized stress versus the normalized buckling length, exhibiting the existence of a minimum stress.

Fig. 3 Schematic illustration of the formation of kinking bands of flat plate under compression.

Fig. 4 The normalized delamination stress as a function of the normalized interlaminar surface energy for thin-walled tube.

Fig. 5 The normalized kinking stress versus the normalized initial misalignment angle.

Fig. 6 The failure strength due to two different mechanisms, the formation of kinking bands and interlaminar delamination. The two failure processes are competing against each other.

Fig. 7 Failure mechanisms map showing regions dominated by different failure modes.

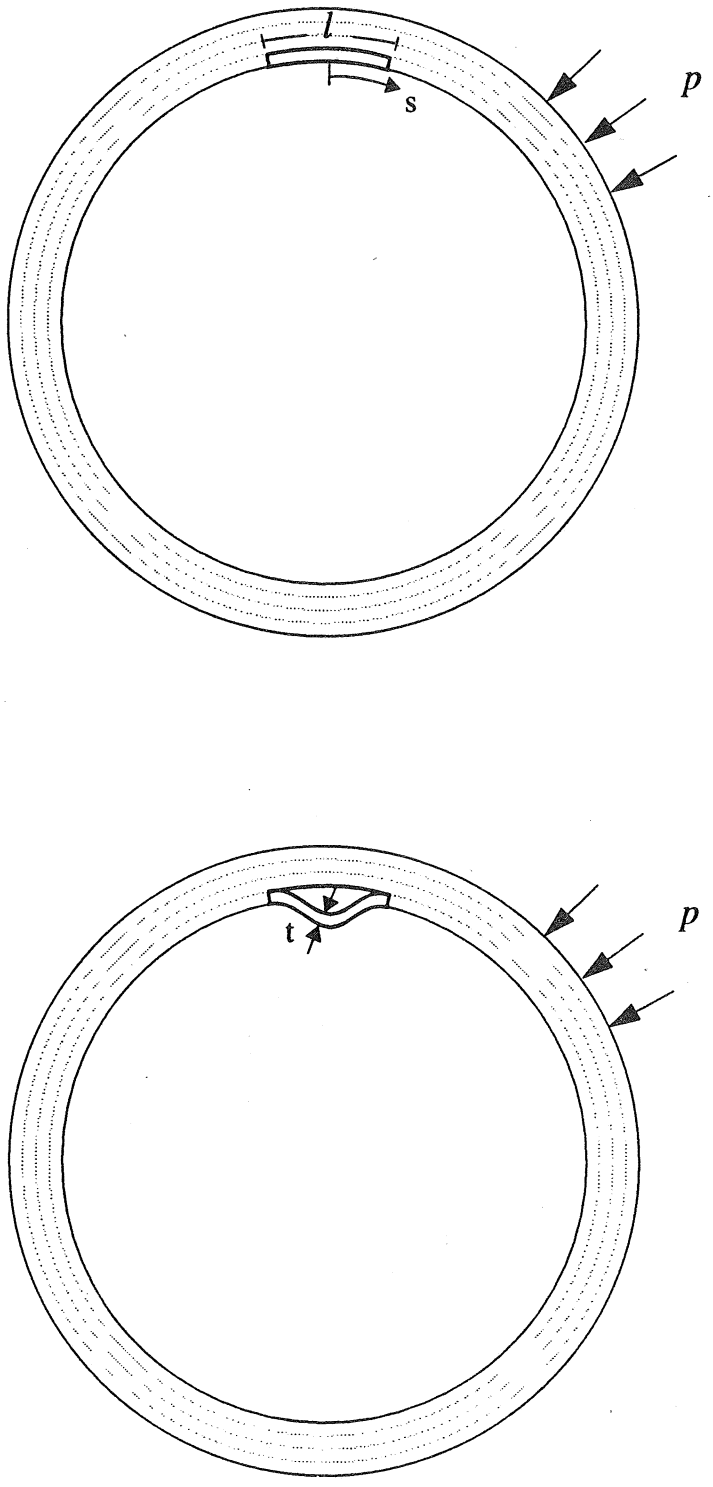

Fig. 1

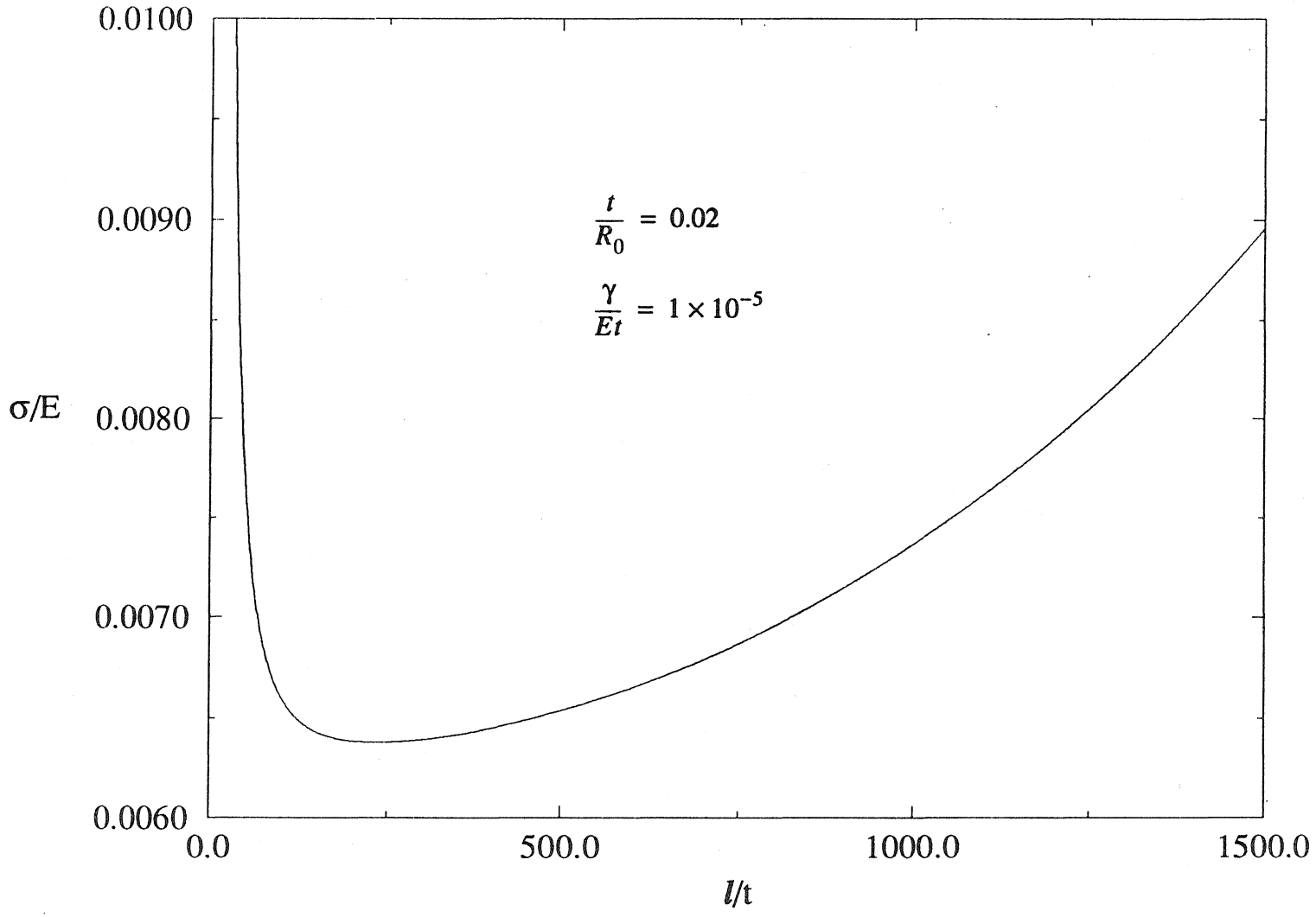
0.0100
0.0090
0.0080
0.0070
0.0060
σ/E
$\frac{t}{R_0} = 0.02$
$\frac{\gamma}{Et} = 1 \times 10^{-5}$
0.0
500.0
1000.0
1500.0
l/t

Fig. 2

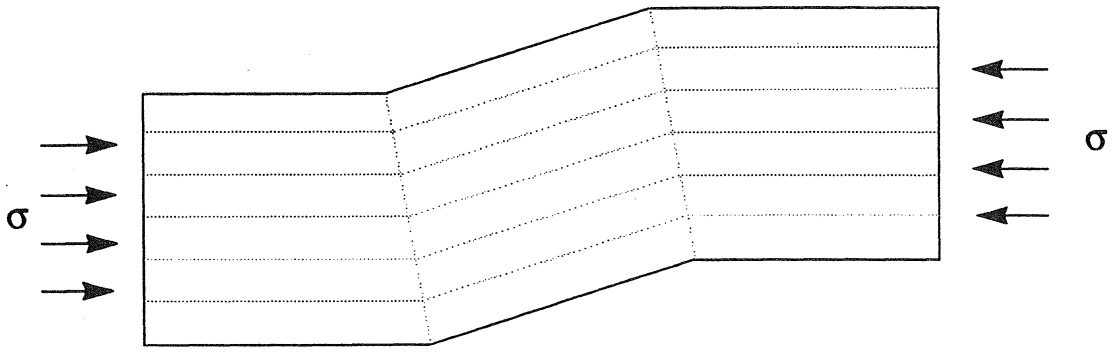

Fig. 3

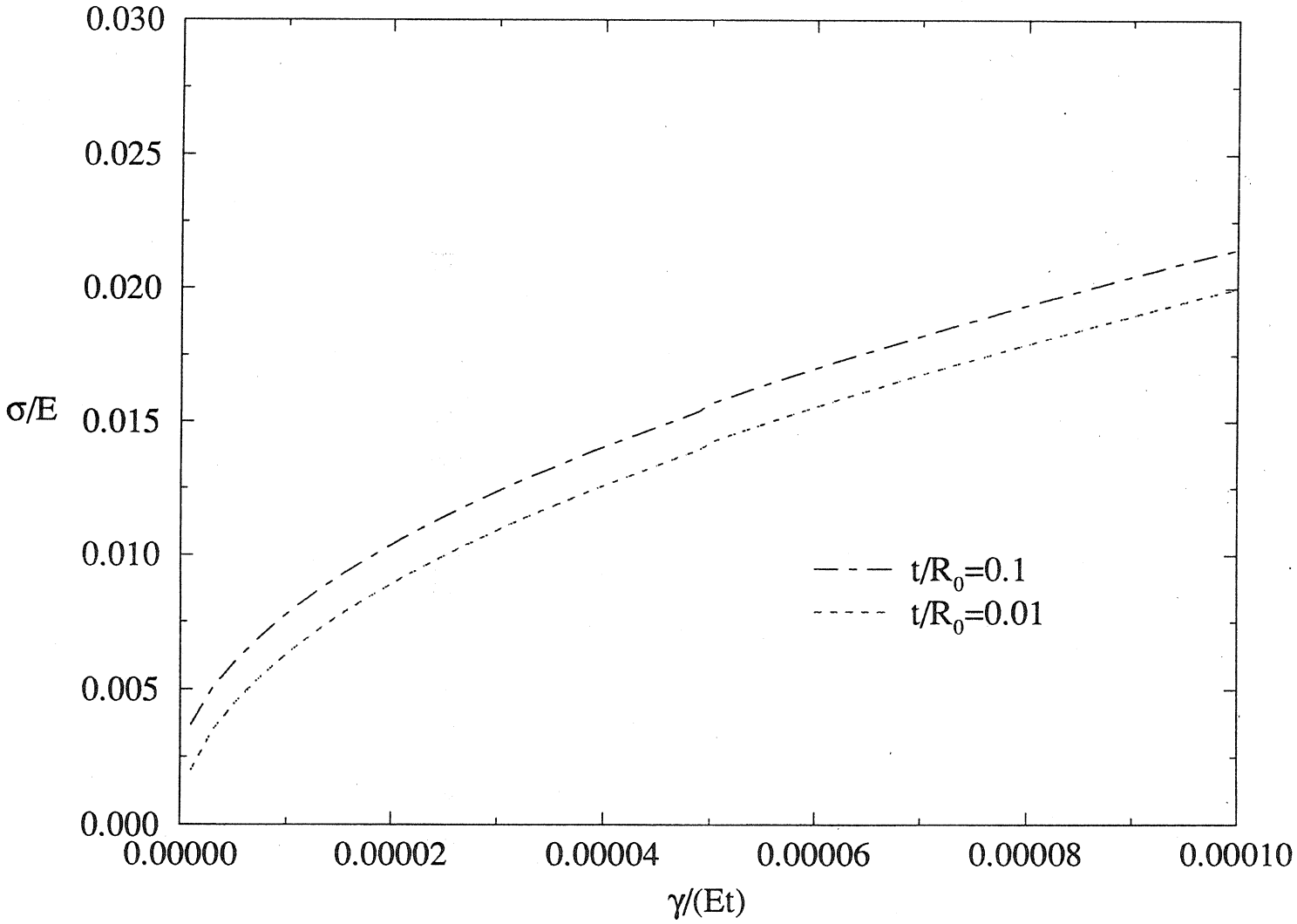
0.030
0.025
0.020
0.015
0.010
0.005
0.000
σ/E
0.00000
0.00002
0.00004
0.00006
0.00008
0.00010
γ/(Et)
t/R0=0.1
t/R0=0.01

Fig. 4

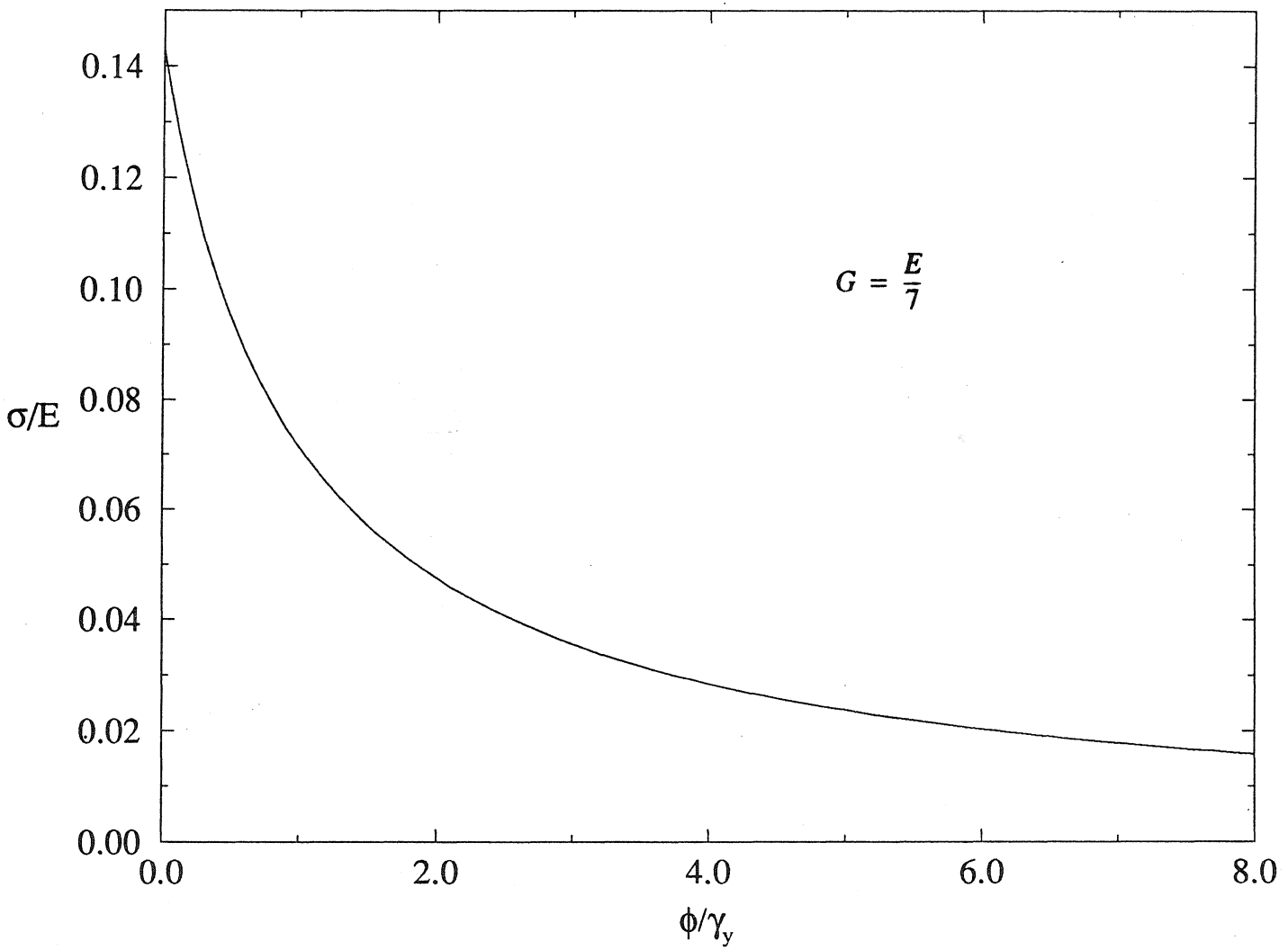

Fig. 5

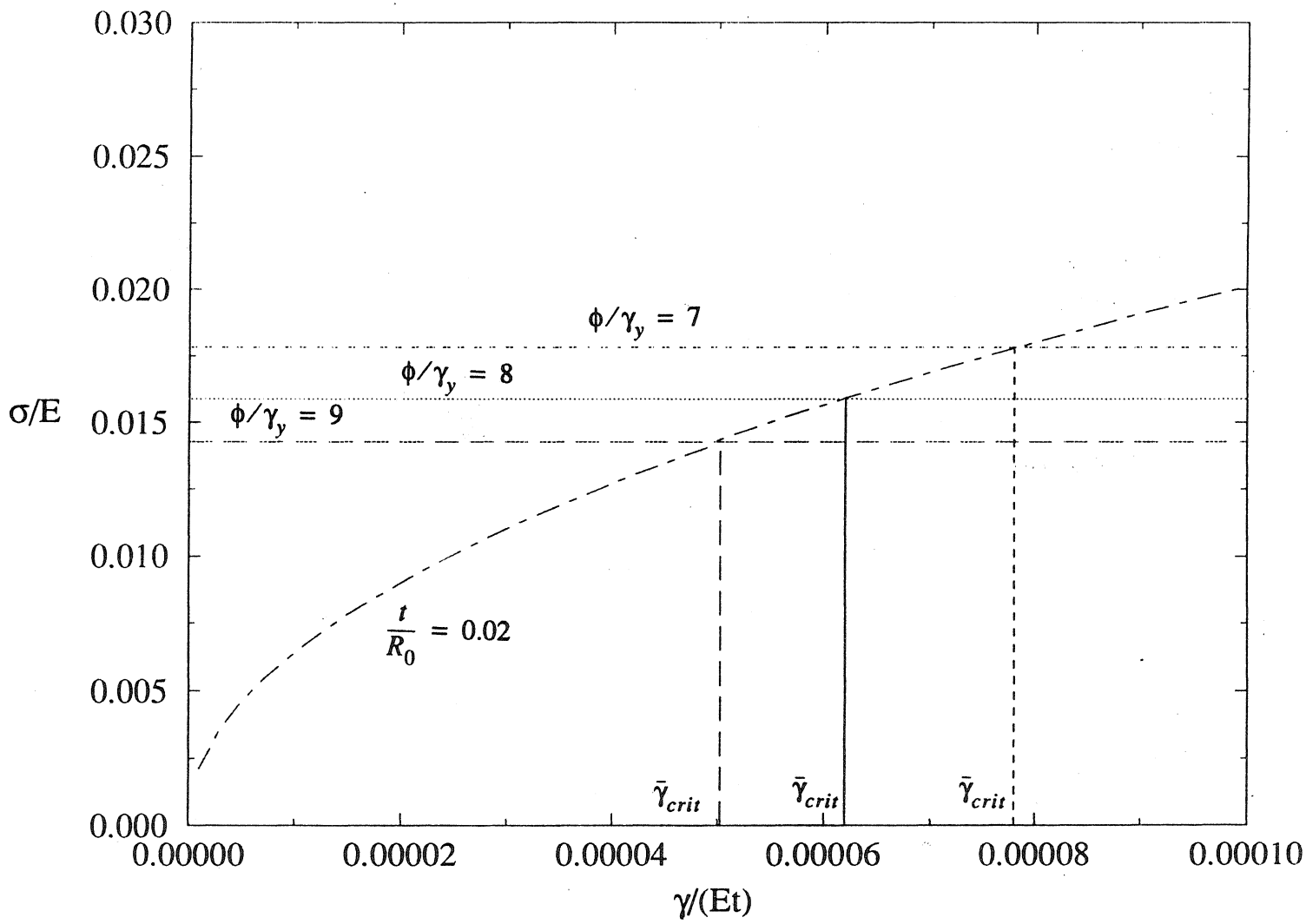
0.030
0.025
0.020
0.015
0.010
0.005
0.000
σ/E
φ/γ_y = 7
φ/γ_y = 8
φ/γ_y = 9
t/R_0 = 0.02
γ̄_crit
γ̄_crit
γ̄_crit
0.00000
0.00002
0.00004
0.00006
0.00008
0.00010
γ/(Et)

Fig. 6

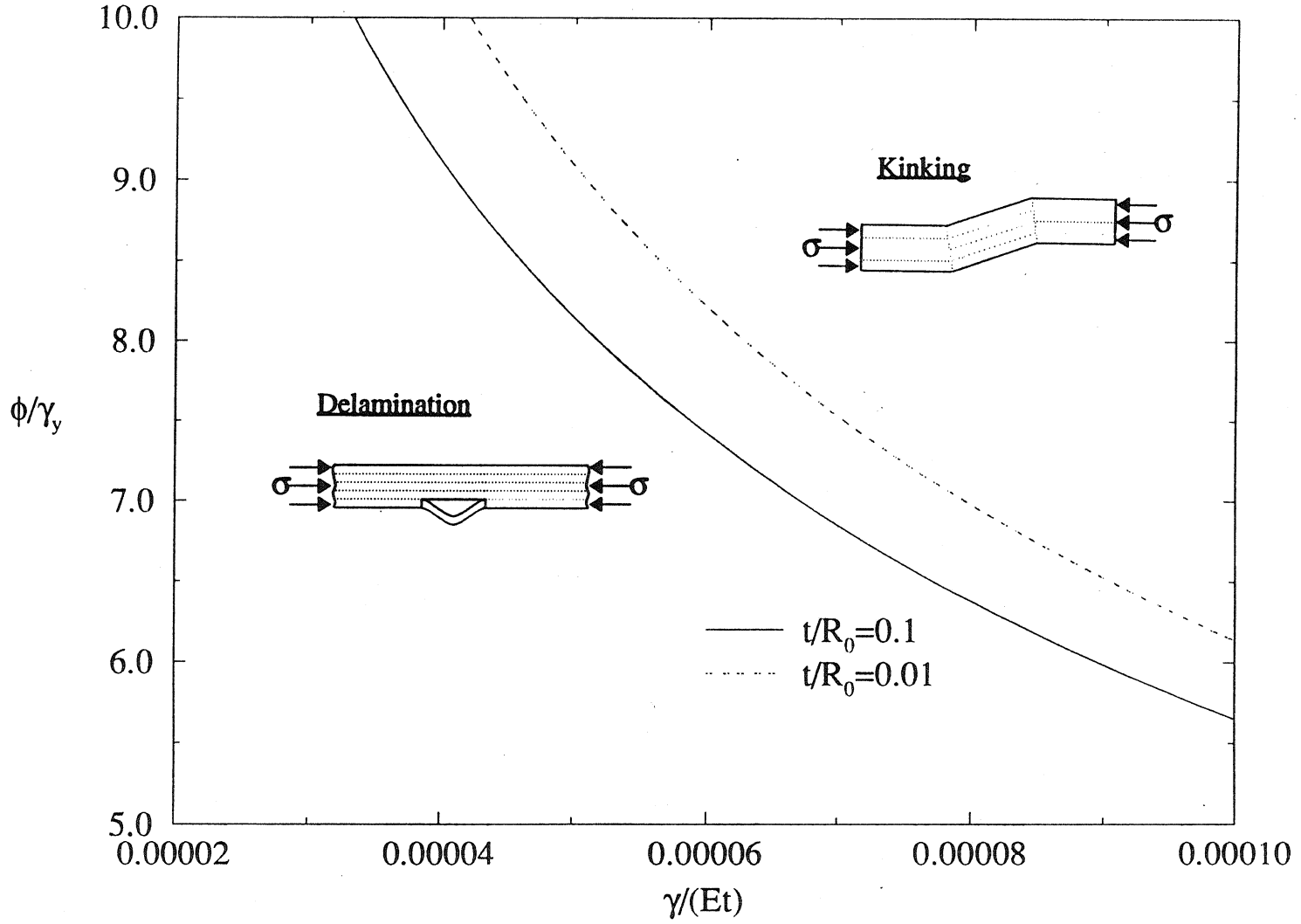
10.0
9.0
8.0
7.0
6.0
5.0
ϕ/γ_y
0.00002
0.00004
0.00006
0.00008
0.00010
$\gamma/(Et)$
Kinking
σ
σ
Delamination
σ
σ
t/R_0=0.1
t/R_0=0.01

Fig. 7